# Integration of Pressure-Transient Data in Modeling Tengiz Field, Kazakhstan—A New Way To Characterize Fractured Reservoirs

**Yan Pan, Mun-Hong Hui, Wayne Narr, Gregory King,** and **Terrell H. Tankersley,** Chevron; **Steve D. Jenkins,** KPO; and **Eric A. Flodin, Philip W. Bateman, Chris Laidlaw,** and **Hai Xuan Vo,** Chevron

## Summary

A systematic work-flow to integrate pressure-transient data collected from single-well buildup tests in numerical reservoir-simulation models for a fracture/matrix system is presented. The results of its application in a sector model in the southeast region of Tengiz field in Kazakhstan are also discussed.

The procedure starts with a selected numerical-simulation model, either a discrete fracture/matrix (DFM) model or a dual-porosity dual-permeability (DPDK) model, and follows with the analysis of a numerically generated buildup test to calculate the fracture spacing and shape factor of the model. Then, following the correlations between pressure-transient-analysis results and the average or representative values of the model-input parameters near the well, which contain the previously obtained fracture spacing and shape factor, the numerical-model parameters are adjusted in each iteration to match the pressure-transient behavior observed in the buildup test including the interporosity flow between matrix and fracture and the radial flow in the total system.

Before field application, the numerical-simulation results from both DFM and DPDK models were validated against analytical pressure-transient solutions for a dual-porosity system. The gridding and time-steps were calibrated to reproduce the analytical transient behavior. Finally, the new work-flow was applied to a sector model of Tengiz field in the southeast region focusing on two wells. Following the developed work-flow, a DFM model was constructed, and its fracture and matrix properties were adjusted to honor buildup-test data at both wells and the transient data collected during a pulse test conducted between them. The study results show that the key factors of a DFM model on buildup transient response are the fracture permeability, fracture aperture, and matrix permeability in the well-drainage area, and the dominant parameters on pulse-test response are the fracture permeability and matrix porosity in the influence area between the two wells. Using the correlations quantitatively for each simulation step could reduce the total number of iterations needed to converge to the numerical solution. The modified model also generated flow distribution along the wellbore, consistent with production-logging data at one well. The resulting sector map of pressure change during buildup test indicates the area with well-connected fracture network. Dynamic transient data contain rich information about reservoirs, and the effective integration of dynamic and static data would have a big impact on reservoir management by potentially minimizing the number of wells to be drilled, maximizing the production, and optimizing recovery.

The novelty of this study is the quantitative use of the correlations between pressure-transient-analysis results and the representative values of the input parameters in a numerical model to reduce the number of simulation iterations. Its application in Tengiz is also one of the rare examples in which single-well and multiple-well transient data, production logging, and image-log data are all available.

## Introduction

Reservoir characterization is an important component of reservoir management. The characterization process integrates information from two main sources: static data (such as geological interpretation that is based on outcrop, seismic, well log, core, drilling-fluid loss) and dynamic data (such as well test, production logging, and production history). Although the use of dynamic data in the reservoir-characterization process was attempted in the past, its application is still limited and lacking a robust work-flow. In this study, numerical well-testing techniques (Kamal et al. 2005) were applied to understand and characterize the fracture/matrix properties of naturally fractured reservoirs (NFRs), which are especially challenging because of their often-extreme heterogeneity and, thus, high degree of flow-related uncertainty (Narr et al. 2006). The effective usage of pressure-transient data that contain rich information about wells and reservoir should narrow the uncertainty, improve the characterization, and help optimize field development.

An NFR has a network of permeability-enhancing fractures that separate matrix. The flow-simulation models used most commonly for NFRs are single-porosity enhanced-permeability models, dual-porosity (DP) models, and DPDK models. Other less-commonly used methods include discrete-fracture-network (DFN) models and DFM models. The DP model is derived from the conceptual model proposed by Barenblatt et al. (1960) and Warren and Root (1963). In this model, the reservoir consists of two interacting media: a uniformly distributed network of low-volume but highly conductive fractures and isolated matrix blocks that contain the bulk of pore volume (PV). In a DFM model, relatively more-realistic geometry, orientation, density, and other properties of fractures could be considered by using the geological information acquired during exploration and development of reservoirs explicitly (Wei et al. 1998; Casciano et al. 2004; Karimi-Fard et al. 2004; Basquet et al. 2005; Sarma and Aziz 2006; Casabianca et al. 2007; Rogers et al. 2007; Hui et al. 2007, 2008; Izadi and Yildiz 2009).

Conventionally, the analytical models that treat the reservoirs as simplistic and idealized abstractions are used for evaluating pressure-transient-test data. These models may not be representative for real complex heterogeneous reservoirs. However, the obtained analysis results, such as the estimations of formation permeability, the storativity ratio, and interporosity flow coefficients of a DP model, are valid, effective average properties of the reservoir within the tested volume near a well. The analytical solutions of pressure-transient responses for NFRs were built on DP models (Warren and Root 1963). Depending on the flow conditions when the interporosity flow from the matrix system into the fracture network occurs, there are two types of analytical solutions: pseudosteady-state and transient. The analytical pseudosteady-state

Copyright © 2016 Society of Petroleum Engineers

This paper (SPE 165322) was accepted for presentation at the SPE Western Regional & AAPG Pacific Section Meeting Joint Technical Conference, Monterey, California, USA, 19–25 April 2013, and revised for publication. Original manuscript received for review 14 January 2014. Revised manuscript received for review 11 August 2015. Paper peer approved 29 October 2015.

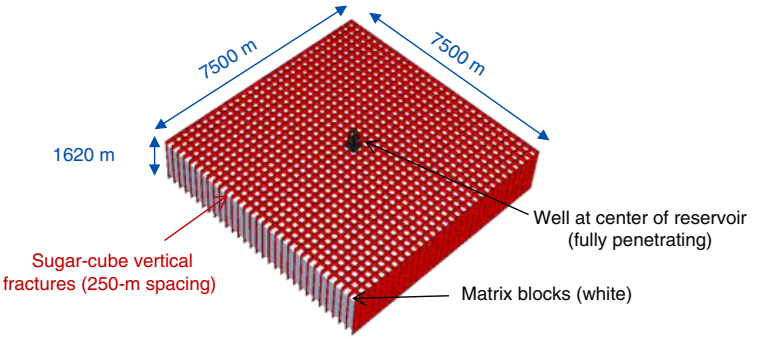


**Fig. 1—A reservoir with uniform sugar-cube vertical fractures and a vertical well at the center.**

solution for NFRs has a distinct signature on the pressure response characterized by a symmetric trough on the pressure-derivative curve in the log-log diagnosis plot, whereas the transient solution may not show a well-defined trough. The property contrast between fracture network and matrix system and their configuration determine whether the interporosity flow is pseudosteady or transient. Since 1963, many papers were published on fractured-reservoir well-test interpretations and studies. Samaniego-V and Cinco-Ley (2009) give detailed reviews of major works in the literature.

Our work aims at developing a systematic procedure for integrating well-test data that contain rich information on effective reservoir properties in a numerical reservoir model that uses a realistic fracture-system geometric description and natural variability of such fracture-system properties for NFRs. It includes three parts. The first is the validation of numerical solutions from DFM and DPDK models generated with a numerical reservoir simulator against analytical solutions for a DP system. Second, after investigating the impact of different fracture/matrix properties of a numerical model on pressure-transient responses from single-well tests with synthetic cases, based on the results, a work-flow for integration of transient data in NFR models was developed. This procedure uses numerical models to simulate transient-test responses and to compare with collected pressure-transient data. Then, following the correlations between the parameter estimations from transient analysis of the numerical results and the representative or average input parameters near a well in the numerical model, the model-input parameters are adjusted for the next iteration. The steps are repeated until the numerical pressure-transient responses match the measured data. The analytical model used to analyze the numerical responses is the Warren and Root (1963) solution. However, our work-flow can use any analytical or semianalytical solutions as long as they provide valid correlations between the transient-analysis results and numerical model-input parameters to guide quantitatively the transient-data-matching process. In the third part, this approach was applied in a realistic DFM sector model for the Tengiz oil field. The ultimate goal of our study is to use pressure-transient data from buildup tests at individual wells and from pulse tests among multiple wells in a real field to build and update the numerical reservoir models. The updated models, which incorporate both realistic geological static data and actual field dynamic data, are expected to be more robust and predictive to assist reservoir management.

| Parameter | Value | Units |
|---|---|---|
| Reservoir geometry | 7500 by 7500 | m |
| Formation thickness, $h$ | 1620 | m |
| Fracture spacing, $x_m$ | 250 | m |
| Matrix porosity, $\phi$ | 0.01 | |
| Matrix permeability, $k_m$ | 0.01 | md |
| Fracture permeability, $k_f$ | 1,000 | md |
| Fracture aperture, $a_f$ | 0.02 | m |
| Well radius, $r_w$ | 0.0823 | m |
| Well skin factor, $s$ | 0 | |
| Wellbore storage, $C$ | 0 | bbl/psi$^{-1}$ |
| Initial reservoir pressure | 10,000 | psia |

Table 1—Properties of a uniform sugar-cube DP reservoir.

## Calibration and Validation

To fully understand the pressure-transient behavior of different numerical reservoir models and to calibrate the gridding selection and simulation time-steps, a validation step was taken first with synthetic cases. Because horizontal fractures are usually not observed in the reservoir below moderate depth, a fully penetrating vertical well at the center of a single-layer sugar-cube DP reservoir with only vertical fractures was considered **(Fig. 1).** The fracture network is composed of two orthogonal sets of vertical fractures as long as the reservoir size with a constant spacing of 250 m. Matrix blocks fill the space between the fracture planes. The uniform fracture and matrix properties are shown in **Table 1.** A black-oil formulation was selected to represent the fluids. A drawdown test (3,500 days) at a constant oil-production rate of 5,000 STB/D was simulated numerically with both DFM and DP models, and the pressure responses were compared with analytical solutions.

For our numerical models with uniform fracture and matrix properties, the effective properties were calculated with the following equations.

- Effective permeability of a DP system,

$$k^{\text{eff}} = \frac{(x_m \cdot k_m + a_f \cdot k_f)}{(x_m + a_f)}. \quad \ldots\ldots\ldots\ldots\ldots\ldots (1)$$

- Storativity ratio of fracture to the total system,

$$\omega = \frac{\phi_f \cdot c_{tf}}{\phi_f \cdot c_{tf} + \phi_m \cdot c_{tm}}. \quad \ldots\ldots\ldots\ldots\ldots\ldots (2)$$

- Interporosity flow coefficient,

$$\lambda = \frac{\alpha}{x_m^2} \cdot \frac{k_m}{k_f^{\text{eff}}} \cdot r_w^2; \quad k_f^{\text{eff}} = \frac{k_f \cdot a_f}{x_m + a_f}; \quad \lambda = \frac{KSIGMA \cdot r_w^2}{k_f^{\text{eff}}}. \quad \ldots\ldots\ldots\ldots\ldots\ldots (3)$$

Parameter $\alpha$ is the geometric shape factor that describes the contact surface area between matrix blocks and fracture network. For a sugar-cube DP system with 2D fractures, the value of $\alpha$ is 16 according to the Coats (1989) formula and 19.7 from Lim and Aziz (1995). Our numerical results showed $\alpha$ is closer to 16 for this synthetic case. For field cases with relatively realistic realizations in which matrix blocks have irregular shape and fracture distribution varies, the shape factor can be obtained by analyzing the numerical transient response and compare with model input, which will be discussed in the next section. The interporosity flow

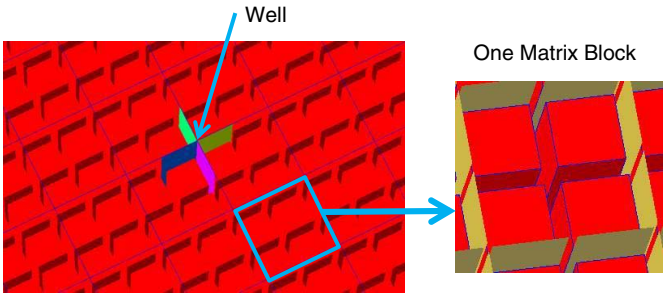


**Fig. 2—The well location and first-level grid refinement in a DFM model for a uniform sugar-cube reservoir with vertical fractures.**

coefficient $\lambda$ is a function of matrix permeability $k_m$, and the effective permeability of the fracture network $k_f^{\text{eff}}$, which depends on individual fracture permeability $k_f$, aperture $a_f$, and fracture spacing $x_m$. KSIGMA is a parameter used in numerical simulation to describe the transmissibility between matrix and fracture network.

The numerically simulated drawdown-test pressure responses were analyzed with analytical DP models, and the estimated parameter values were compared with those calculated directly with Eqs. 1 through 3.

## DFM Model

A synthetic one-layer DFM model with $30 \times 30$ matrix blocks and $31 \times 31$ fully penetrated vertical fractures as long as the reservoir size with a fully penetrated vertical well at the center of the reservoir was created to simulate the drawdown test in the sugar-cube DP system. The well was in the intersection point of two fractures and surrounded by four matrix blocks. An unstructured grid with one level of grid-refinement, four gridblocks within each matrix block, and eight fracture segments surrounding the matrix block **(Fig. 2)** was used. The minimum time-step was selected as 1 hour for the 3,500-day test, and increased logarithmically based on transient behavior. The pressure responses during the drawdown test simulated by the DFM (green curve) and those of the analytical solution (red) are shown in **Fig. 3a,** and the log-log plot of pressure change and pressure derivative are shown in Fig. 3b. The horizontal portion of the pressure derivative (lower curve) from 2,000 to 40,000 hours indicates the second radial-flow period, from which the effective permeability of the DP system can be estimated. The separation between the pressure (upper curve) and the pressure derivative (lower curve) during the radial-flow period provides an estimate of well skin factor. The trough between 20 and 2,000 hours is the interporosity flow period, when fluid starts to flow out of matrix blocks into the fracture network. From the depth of the trough in the pressure-derivative curve, the storativity ratio of the fractures to the total system $\omega$ can be obtained. The interporosity flow coefficient $\lambda$, which is an indication of how easy or difficult it is for fluids to flow out of low-permeability matrix and enter the high-conductivity fracture network, can be estimated from the time when the trough ends and the second-radial flow period starts (2,000 hours). After 40,000 hours, the pressure derivative shows pseudosteady-state flow behavior (unit-slope straight line) caused by the finite size of the reservoir. For ideal DP transient behavior (with very low wellbore storage and small or negative skin), there should be a first radial-flow period at early time governed by flow only inside the fracture network before the onset of interporosity flow. The simulated response of the DFM (green in Fig. 3b) shows linear flow before 10 hours because of the fractures crossing the wellbore in the DFM, and the first radial flow is thus not observed. Nevertheless, the analytical solution (red in Fig. 3b) assuming no wellbore storage was reasonably matched by the numerical-simulation results from DFM (green).

**Table 2** shows that the DP-system properties calculated from Eqs. 1 through 3 are reasonably consistent with the analysis results of the numerical DFM pressure response. The difference in permeability is negligible. The difference in interporosity coefficient is less than 14% and within the same scale of $10^{-7}$. The difference in storativity is relatively large, 48%. It is challenging to match this parameter. The input well skin factor in the numerical model is zero. The skin value of −6.40 obtained by analyzing the simulated pressure-transient response is actually the equivalent skin, because the well is at the crossing point of two fractures in the DFM model (Fig. 2). The equivalent skin of a 250-m fracture plane crossing this well should be −6.63 according to the

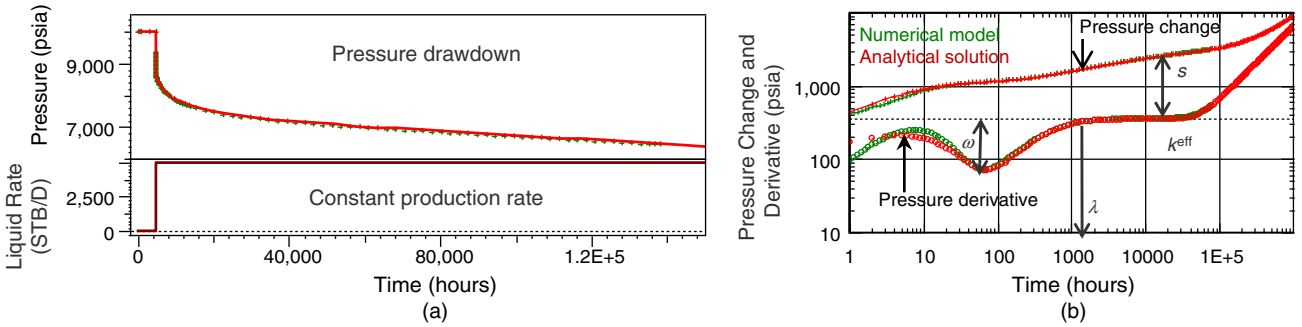


**Fig. 3—Pressure responses during a drawdown test of a vertical well in a sugar-cube DP reservoir with DFM model.**

| | Effective System Permeability $k^{\text{eff}}$ (md) | Fracture Storativity Ratio $\omega$ | Interporosity Flow Coefficient $\lambda$ | Well Total Skin $s$ |
|---|---|---|---|---|
| Equations | 0.09 | 0.044 | 2.5E–7 | 0.00 |
| DFM | 0.09 | 0.065 | 2.2E–7 | –6.40 |

Table 2—Numerical results of DFM model for a drawdown test of a vertical well in a sugar-cube DP reservoir.

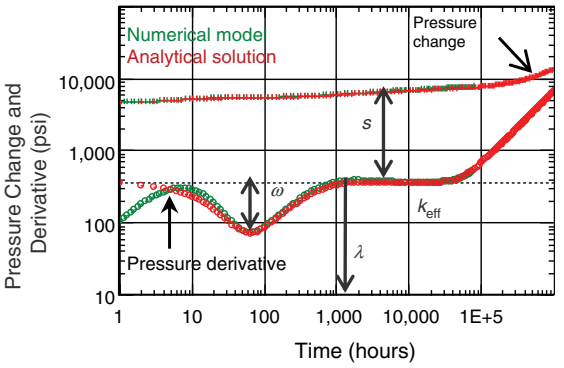


**Fig. 4—Log-log plot of a drawdown test of a vertical well in a sugar-cube DP reservoir with DP model.**

correlation $s_{equiv} = -\ln(L_f/4/r_w)$. If two fractures cross the wellbore, the skin could be smaller than −6.63. Sensitivity study showed that the fracture conductivity and the grid refinement near the wellbore would have impacts on the equivalent skin derived from the transient analysis of the numerical-simulation results with the DFM model. Further details are beyond the scope of this paper.

## DPDK Model

A Cartesian $30 \times 30 \times 1$ DPDK numerical model was also created to simulate the drawdown-test response from the same DP system (Fig. 1). The size of each gridblock was the same as the sugar-cube fracture spacing of $250 \times 250$ m. The well was in the center of a gridblock in the middle of the reservoir. Each gridblock was assigned two sets of uniform properties, one for matrix and the other for fracture. Fractures were not represented explicitly as in the DFM model. The drawdown-simulation results are shown in **Fig. 4.** The numerical DPDK model (green curves) captured the interporosity flow trough, the second radial-flow, and the late-time pseudosteady-state periods, just as the DFM did, and are consistent with the analytical solution (red curves) starting from 10 hours. The early-time (<10 hours) first radial flow was not observed in the numerical response because of the large wellblock size of $250 \times 250$ m. **Table 3** shows that the DP properties calculated from Eqs. 1 through 3 are reasonably consistent with the analysis results of the numerical DP pressure response.

The DFM model provides a skin factor of −6.40 (Table 2), which represents the equivalent skin caused by a well crossing two vertical fractures. The DP model, which homogenizes the fractures in a DP sense, does not exhibit this feature; it gives a skin factor of −0.46, which is close to the input value of 0.0. One should use this observation as the guidance when the DFM model is selected for a numerical well-testing study. The skin effect seen from DFM response is a combination of well mechanical skin and any fractures crossing the wellbore.

The transient behavior simulated with a DPDK model is sensitive to gridblock size. Different from a single-porosity system in which finer Cartesian gridlines close to following streamlines simulate more-accurate transient responses, for a DP system, the grid-refinement level has to be selected to balance the need to reproduce early-time transient radial flow, for which a finer grid may be preferred, and the need to generate the interporosity flow between the matrix system and the fracture network, which may require the grid size to be in scale similar to that of the fracture spacing near the well. If there are enough data (e.g., cores, image logs, production log, and analogs) to generate reasonable fracture distributions, for any grid size, the representative gridblock properties, such as fracture porosity and the transmissibility between matrix and fracture, can be calculated based on the discrete fractures within each cell (Hui et al. 2013). Hence, the derived numerical DP model could simulate the interporosity flow behavior as observed during transient tests without relying on a particular grid size.

## Work-Flow To Integrate Single-Well Transient-Test Data for NFR

Following the calibration and verification process of numerical-simulation models, a sensitivity study of fracture/matrix system parameters on pressure-transient responses was conducted. Based on the study results, a systematic procedure of incorporating single-well transient-test (buildup or drawdown) data in discrete-fracture simulation models was developed. The goal is for any given numerical discrete-fracture model to adjust the selected-model input parameters to make the numerically simulated transient-test responses match the measured-pressure data at wells. The transient-analysis results with any selected analytical solutions are not used directly in the numerical model. Only the correlations between the transient-analysis results and the numerical-model input parameters, Eqs. 1 through 3, are used to quantitatively guide the selection of input parameters for each iteration during the process. The work-flow is shown in **Fig. 5.**

The systematic procedure is as follows:

1. Select the most likely fracture realization based on geological information, such as well logs, cores, image logs, outcrop analogs, and dynamic flow data, such as from production logging tool (PLT) and lost circulation. In the current study, fracture properties, such as aperture and permeability, are assumed uniform for each discrete fracture, although properties could vary among different fractures. At this step, the fracture sizes, orientations, and spatial distribution are specified, and are combined with the reservoir structure, such as bed dipping and pinchout.
2. Generate an unstructured grid that represents the fracture realization defined in the previous step (Hui et al. 2008). Choose the base-case fracture-matrix system properties, such as matrix permeability and porosity, and fracture permeability and aperture, according to information in hand (static-data interpretation and well-test-analysis results). The properties can be heterogeneous, and modifiers can be used to adjust its properties. Load the fluid PVT properties and the production/injection history into the simulation model. Select the appropriate grid-refinement level near the wellbore and time-steps (Kamal et al. 2005). Run this base-case numerical simulation of the transient test.
3. Compare the simulated buildup/drawdown pressure response at the well with the gauge data collected during the transient test. Pressures may need to be adjusted to the same datum as the gauge depth for comparison. If the numerical results match gauge data during the transient test in both Cartesian history plot and transient diagnosis log-log plot, the base case is one solution. If not, proceed to the next step.
4. Analyze the simulated transient-test pressure response and estimate the effective permeability of the fracture-matrix system $k^{eff}$, fracture storativity ratio $\omega$, and interporosity flow coefficient $\lambda$.

| | Effective System Permeability $k^{eff}$ (md) | Fracture Storativity Ratio $\omega$ | Interporosity Flow Coefficient $\lambda$ | Well Skin $s$ |
|---|---|---|---|---|
| Equations | 0.09 | 0.044 | 2.5E–7 | 0.00 |
| DP Model | 0.09 | 0.050 | 2.0E–7 | –0.46 |

Table 3—Numerical results of Cartesian DP model for a drawdown test of a vertical well in a sugar-cube DP reservoir.

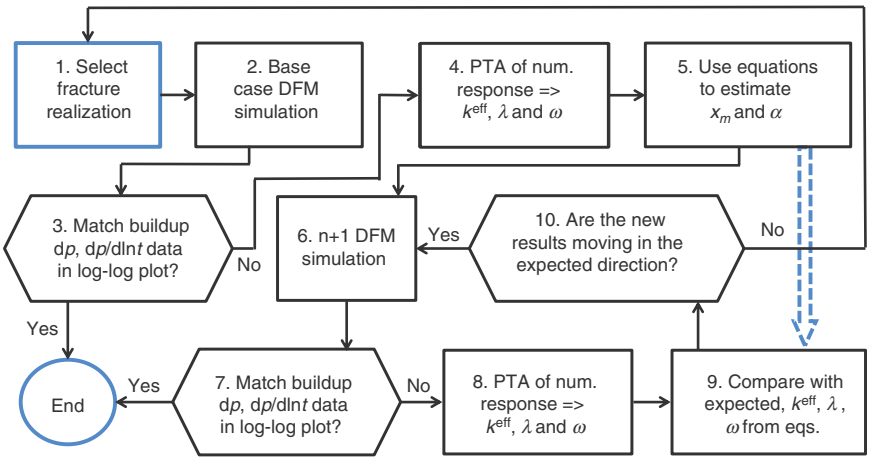


**Fig. 5—The work-flow of single-well transient-test-data integration for NFR.**

5. Use these estimates and those average or representative values of the input parameters ($k_m$, $\phi_m$, $k_f$, $a_f$) near the well in numerical model in Eqs. 1 through 3 to calculate fracture spacing $x_m$ and geometric shape factor $\alpha$ of the current fracture realization. Different realizations may produce different fracture spacing and shape-factor values. These two values together with geological information (e.g., reservoir structure, fracture-size distribution, spatial distribution, number of fracture sets, and fracture orientation) will be used to guide the following numerical-simulation iterations.
6. Depending on the deviation of the base-case transient response from the test measurements, and following the correlations in Eqs. 1 through 3, select the second set of model parameters to run the simulation.
7. Compare the simulated transient-pressure response at the well with the test measurements. If the numerical results match gauge data well in both the Cartesian history plot and the transient-diagnosis log-log plot, the current case is one solution. If not, proceed to the next step.
8. Analyze the new simulated transient responses.
9. Compare the analysis results with the expected values of fracture/matrix system properties ($k^{eff}$, $\omega$, $\lambda$) from Eqs. 1 through 3 with the average values of current model-input parameters and the values of $x_m$ and $\alpha$ obtained in Step 4.
10. Are the new analysis results moving in a direction consistent with expected values and in relatively similar scale?
11. If "Yes," keep current fracture realization, from the current-analysis results and the expected values; use correlations to quantitatively guide the calculation of the model-input parameters for next iteration. Repeat Steps 6 through 10 until the simulated responses match test data.
12. If "No," generate a new fracture realization to change fracture connectivity (e.g., bigger fracture height/length and adding more fractures) within the bounds of accepted geological uncertainty around the subject well; then repeat Steps 1 through 10.

This work-flow was developed with DFM models as the illustration, but a similar procedure can also be used for DPDK models.

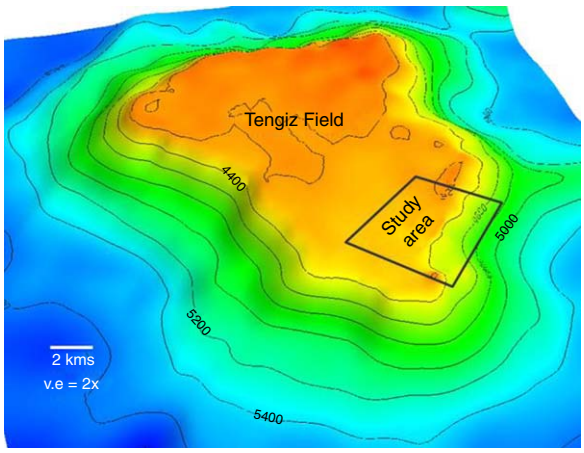


**Fig. 6—Tengiz field structure and the pilot region.**

## Application in Tengiz Southeast-Sector Model

The developed work-flow was applied in a pilot region in Tengiz field. Tengiz is a supergiant oil field with approximately 30 billion STB of original oil in place in the Pricaspian basin of western Kazakhstan. The field produces from an isolated carbonate platform of Devonian-to-Pennsylvanian age, with a flat-lying central platform surrounded by a relatively steep depositional slope **(Fig. 6).** Fractures are common, and they significantly enhance productivity in the outer platform and slope. The reservoir has multiple layers with distinguishable properties. The matrix system is heterogeneous. Most fractures dip steeply and show a wide range of properties (Tankersley et al. 2010; Collins et al. 2013).

Pressure-buildup tests were conducted at more than 100 wells in Tengiz. In the slope area where fractures are common, 70% of the tests detected possible DP behavior with observed radial-flow regime and recognizable trough showing at least the lowest point of the trough and either the beginning or the end of interporosity flow period. Some tests observed textbook DP behavior completed with first radial flow, well-defined symmetric trough (pseudosteady-state interporosity flow), and second radial flow. For test data without recognizable trough, there are several possibilities: The interporosity flow near the well might happen very quickly masked by wellbore storage; it might occur at a later time beyond the test duration; it might be in transient state without recognizable trough; it might be masked by linear flow if the well was drilled crossing an existing natural vertical fracture; or the well was drilled in an area with low fracture density. Because of the high degree of heterogeneity of naturally fractured system, the absence of distinguished trough in transient data is not uncommon in many carbonate reservoirs. If the collected data show any sign of interporosity flow, pseudosteady-state or transient, the integration process is the same. Otherwise, a combination of all parameters is used to match the measured data as any other history-matching process. However, the results may have higher uncertainty because of the difficulty in distinguishing the impacts of different matrix and fracture properties in this case.

Many wells in Tengiz are equipped with permanent downhole gauges; together with oil production, long-term pressure and rate data were also analyzed to characterize the reservoir. One of the

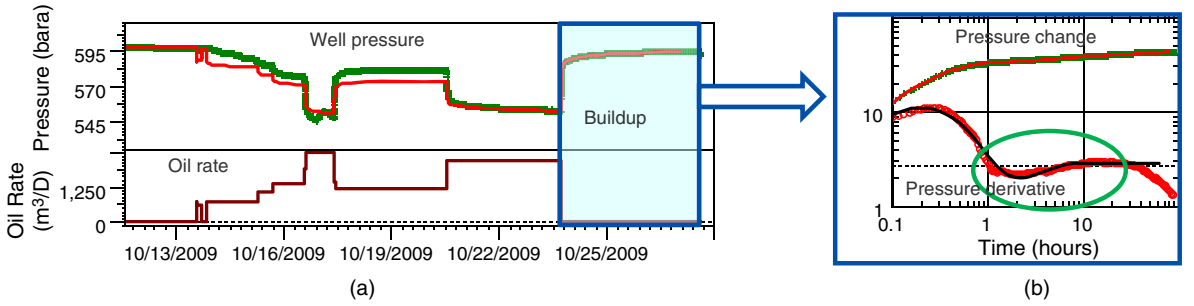


**Fig. 7—History plot (a) and buildup log-log plot (b) of well test conducted at T-1 in October 2009.**

| | DFM Input Parameters | | | | Equations | | | Analysis | | |
|---|---|---|---|---|---|---|---|---|---|---|
| | Average $k_m$ (md) | Average $\phi_m$ | $k_f$ (md) | $a_f$ (m) | $k^{eff}$ (md) | $\omega$ | $\lambda$ | $k^{eff}$ (md) | $\omega$ | $\lambda$ |
| Data | | | | | | | | 3.30 | 0.22 | 2.8E–6 |
| Case 1 | 0.24 | 0.028 | 1000 | 0.02 | | | | 0.38 | 0.38 | 1.4E–4 |
| Case 2 | 2.40 | 0.028 | 10000 | 0.02 | 3.73 | 0.02 | 3.3E–5 | 2.21 | 0.10 | 3.2E–5 |
| Case 3 | 0.78 | 0.028 | 35904 | 0.02 | 5.56 | 0.02 | 2.9E–6 | 2.49 | 0.12 | 1.4E–5 |
| Case 4 | 0.23 | 0.028 | 28138 | 0.04 | 7.73 | 0.04 | 5.5E–7 | 3.30 | 0.22 | 2.8E–6 |

Table 4—Work-flow application in Tengiz sector DFM model at T-1.

benefits of production-data analysis (PDA) is that it provides the drainage-area estimations of each well, which one can use directly in the dynamic data-integration process. However, in the case of Tengiz, PDA is not effective in capturing the interporosity flow behavior caused by frequently varying rates. The transient part of the rate-normalized pressure data is likely to appear noisy and difficult to pinpoint different flow regimes. Nevertheless, it is a very useful tool to study long-term well performance.

A sector in the southeast slope area was selected as the pilot region (Fig. 6) and extracted out of the current history-matched Tengiz full-field DPDK simulation model (Tankersley et al. 2010 and King et al. 2012), which contains three major wells with available buildup tests, pulse tests in two directions, permanent downhole gauges, production-logging data, image logs, and other well-log data. The buildup tests conducted at these three wells captured DP transient behavior successfully and provided reliable fracture/matrix-system property estimations. The rich data collected in this region make it a good candidate to test the new work-flow of integrating single-well transient well-test data, and procedures that will be developed in the future for incorporating pulse tests among multiple wells.

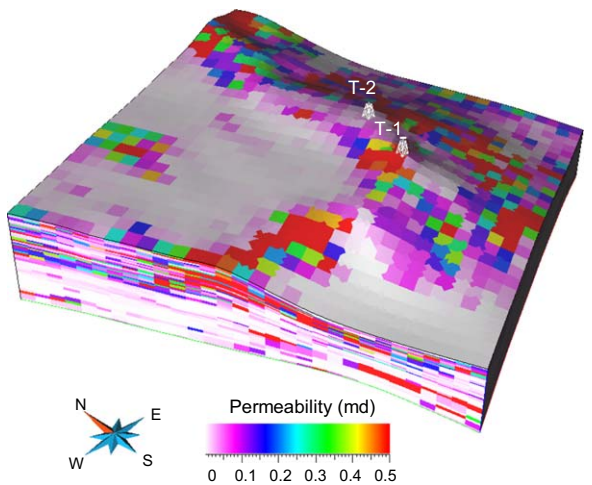


**Fig. 8—Tengiz sector model matrix-permeability distribution.**

## Well Buildup-Test Data

Well T-1 (well names are disguised) was selected as the first well to test the work-flow. A 100-hour buildup test was conducted at this well in October 2009 with controlled flow periods before shut-in **(Fig. 7a).** Data quality is good. As the pressure-derivative curve of the buildup period shows in the diagnosis plot (Fig. 7b), the test detected the interporosity flow from matrix system into fracture network (the trough between 1 hour and 10 hours) followed by the second radial flow (flat derivative between 10 and 30 hours). The late-time data 30 hours after shut-in were influenced by nearby producers that caused the derivative to dive downward. Reliable estimations of reservoir properties ($k^{eff}$, $\omega$, $\lambda$) were obtained **(Table 4).**

## Sector Model

A sector of 7500 × 7500 m with thickness of 1620 m in the southeast pilot region was selected carefully to minimize the influence of the artificial sector boundaries on the buildup-test responses at the subject wells. The sector includes parts of both platform (rather unfractured) and slope (fracture-dominated) areas. The heterogeneous matrix porosity and permeability of the sector were extracted directly from the history-matched full-field Tengiz DPDK model **(Fig. 8).** Water saturation was set to 1% above the water/oil contact (WOC) and 100% below the WOC. The initial pressure field of the sector was taken from the history-matched full-field model at the beginning of the buildup test at T-1 on 13 October 2009 **(Fig. 9).** The matrix and facture could have different pressures at the same time. The sector boundaries were assumed at no-flow condition in current study. Ideally, a material-balance region for the sector can be defined in the full-field model, and sector boundary fluxes can be extracted and specified for sector simulation. Historical rates of other wells in the sector can be carried with simulation. However, we wanted to focus on single-well test integration, and the secondary influence from offset wells was not considered in current study.

## Fracture Distribution

Fracture density is the main variable describing the distribution of fractures throughout the model. It is defined as fracture-surface area per unit volume, and is determined mainly from borehole image logs. Fracture density was distributed throughout the sector area as part of a full-field fracture model with the approach

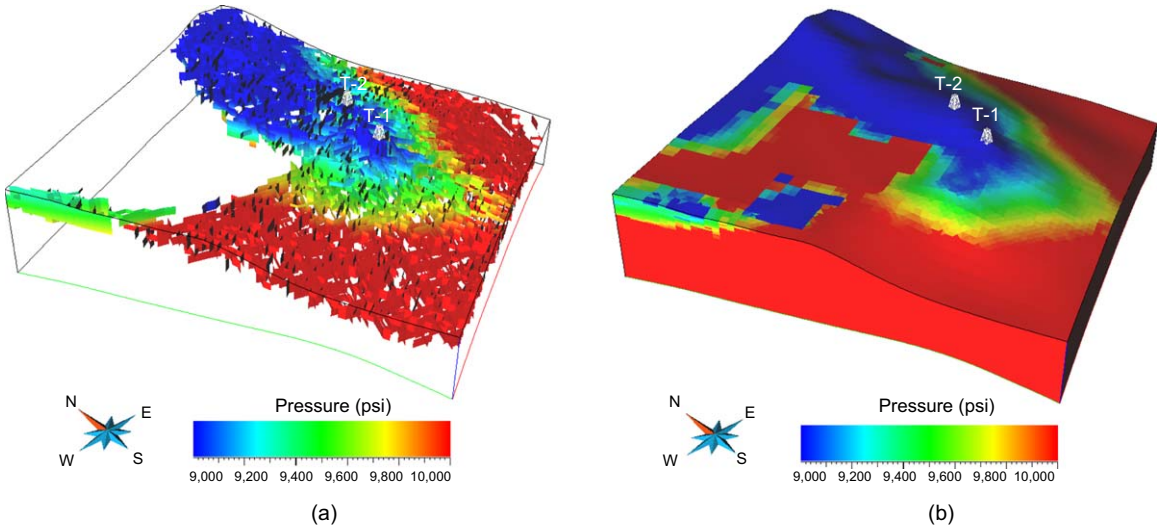


**Fig. 9—Tengiz sector model initial pressure in (a) fracture and (b) matrix.**

described by Tankersley et al. (2010). Fractures typically strike parallel or normal to the local platform-margin orientation.

Based on these spatially explicit geological model properties, a discrete-fracture network model was created with commercial software, in which length, height, and aperture were specified for each fracture set. Two sets of discrete fractures constitute the fracture network—one with orientation that locally parallels the contour of the depositional slope of the reservoir, and the other perpendicular to the first set, which is in accord with both the well data and the character seen at outcrop analogs **(Fig. 10).** To match the limitations of our unstructured grid-handling, fractures are defined to dip parallel to the grid $z$-axis, thereby rendering the fractures to dip vertically in the flow grid. Such steep dip reasonably approximates the character of fractures in the reservoir.

The size of individual fractures cannot be measured directly in a subsurface reservoir; hence, their size distribution is based on studies of fractures in outcrop analogs explicitly to address the Tengiz reservoir (Narr and Flodin 2012). The modeled size of individual fractures is determined stochastically from a specified size distribution. Only "effective fractures" observed in the reservoir are used as a basis for this geological model. Effective fractures are the subset of the total fracture population that show distinct evidence of dynamic response during drilling or logging, such as flow into or out of the wellbore based on PLT, temperature, and lost circulation (Narr et al. 2006; Tankersley et al. 2010). We render just the largest 5% of the effective fracture population as discrete features in our flow-simulation models because of computer-performance limitations. The largest fractures should have the biggest effect on fluid flow in the reservoir. They expose the largest surface area of any fractures to the matrix; they connect across greater distances than small fractures; they are more likely to intersect with other fractures to form percolating networks; and because we define aperture to be proportional to size, they have the largest apertures and, hence, permeability.

The fracture realization was then conditioned to image-log data of selected wells (Fig. 10). The impact of 95% of the smaller fractures that define the remaining component of the total fracture density was incorporated by upscaling them into the "matrix" portion of the simulation model as an effective medium-permeability enhancement, with proprietary software (Tankersley et al. 2010). Based on geological information, static data, and the comparison of the corresponding transient responses, fracture Realization 5 **(Fig. 11)** was chosen as the most-likely fracture distribution. An unstructured grid with one level of grid refinement near wells was generated to reproduce the interporosity flow behavior observed in buildup tests at the wells in the sector **(Fig. 12).**

## Integration of Buildup-Test Data

For the selected fracture distribution, the permeability and aperture were assumed uniform in each discrete fracture. The heterogeneity of fracture system comes from different fracture density in different parts of the sector and different length and height of

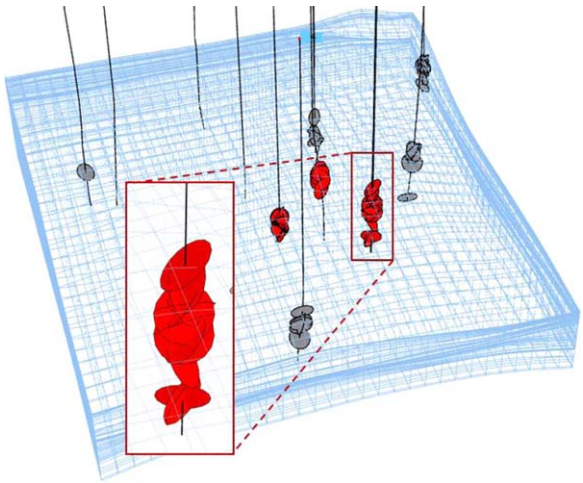

**Fig. 10—Well image-log data used to generate fracture distribution in Tengiz sector model. Disks on wells show locations of effective fractures seen on image logs.**

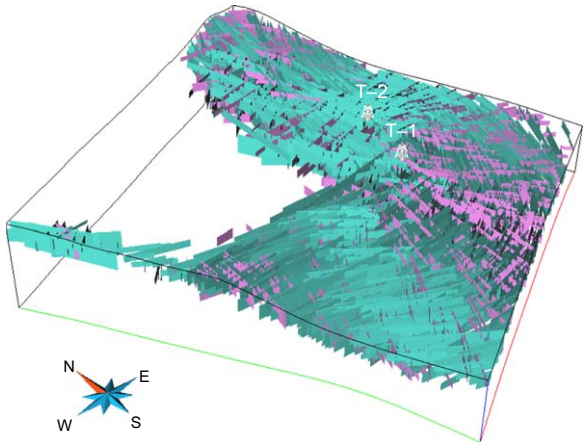


**Fig. 11—Fracture Realization 5 for Tengiz sector model.**

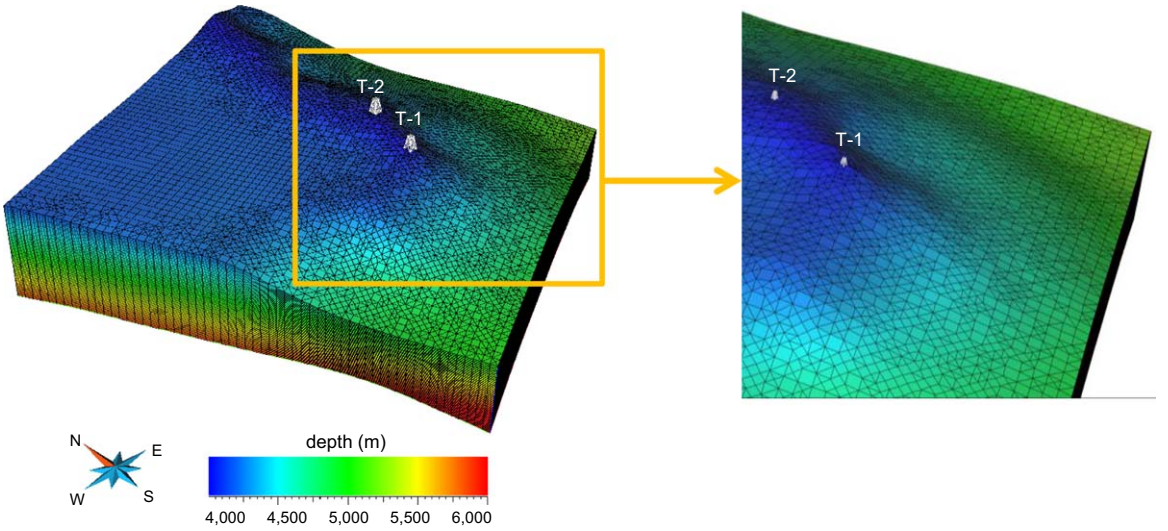


**Fig. 12—Unstructured grid for fracture Realization 5.**

each fracture. The discrete-fracture model variables selected to be adjusted to match pressure-transient data are the multipliers of the heterogeneous matrix permeabilities (the original matrix-permeability distribution remained the same), fracture permeability, and fracture aperture. Following the proposed systematic procedure, the sector-model parameters were adjusted to honor the buildup data collected at T-1 in October 2009. The input parameters used in each case and numerical well-test analysis results are listed in Table 4. The numerical transient responses of each case are shown in **Fig. 13.**

The base case, Case 1, shown as black curves in the log-log plot (Fig. 13b), indicates much lower effective permeability. With the DFM input parameters of Case 1 (Table 4), average $k_m$, $k_f$, and $a_f$ in Eq. 1, the fracture spacing $x_m$ was calculated as 150 m, which is consistent with the average value used to generate fracture Realization 5 near Well T-1. The numerical transient response of Case 1 also indicated earlier interporosity flow than the gauge data (red). With the input parameters of Case 1 in Eq. 3, the shape factor $\alpha$ was estimated at 60 for the current fracture realization near Well T-1. The values of $x_m$ and $\alpha$ were used in the following steps to estimate the model input parameters for next iterations.

Because the effective permeability obtained from Case 1 was 0.38 md, approximately 10 times smaller than 3.3 md derived from gauge data, for Case 2, the fracture permeability $k_f$ was increased from 1,000 to 10,000 md. Its numerical transient-test responses are shown in orange in the same log-log plot (Fig. 13b). With the input parameters of Case 2 and the $x_m$ and $\alpha$ values from Case 1 in Eq. 1, the expected effective permeability was calculated as 3.73 md. The transient analysis of the numerical results estimated $k^{\text{eff}}$ of 2.21 md (Table 4). For realistic heterogeneous reservoirs, Eqs. 1 through 3 are used as correlations to quantitatively guide the selection of the input for next iterations. Because

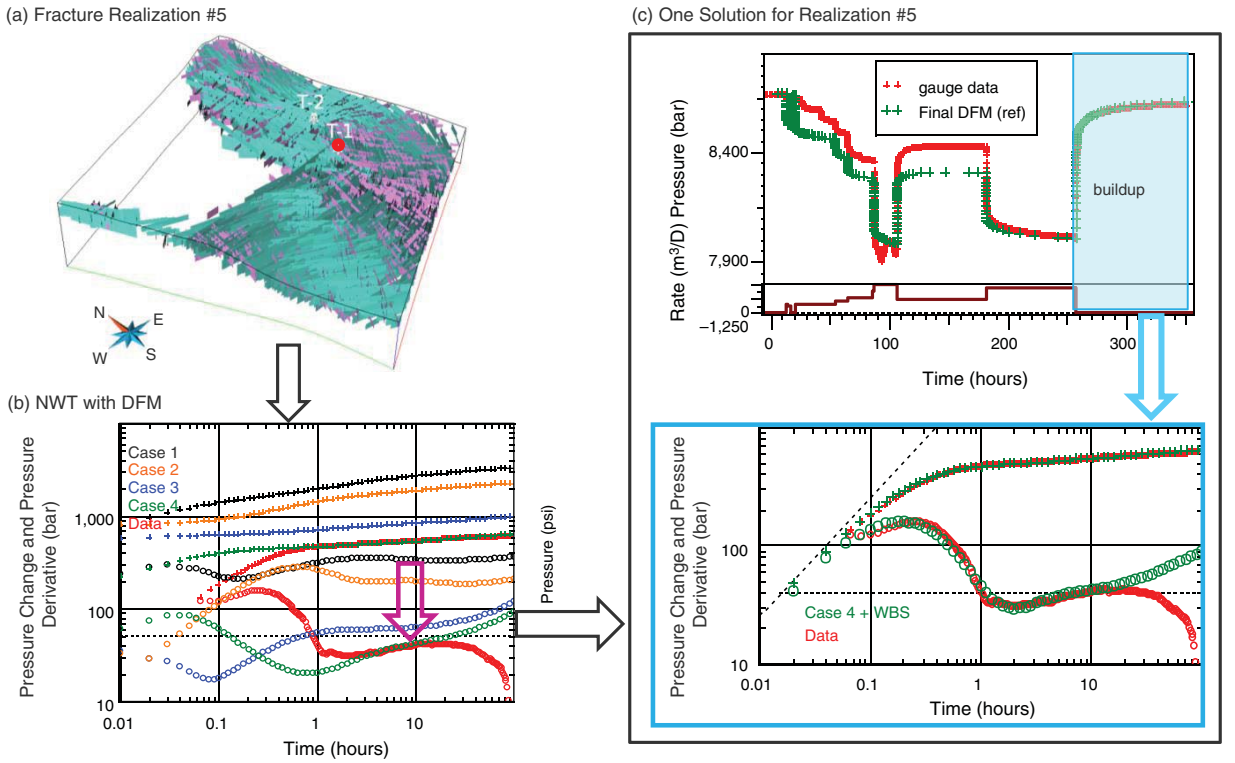


**Fig. 13—A systematic procedure of T-1 buildup integration in Tengiz model.**

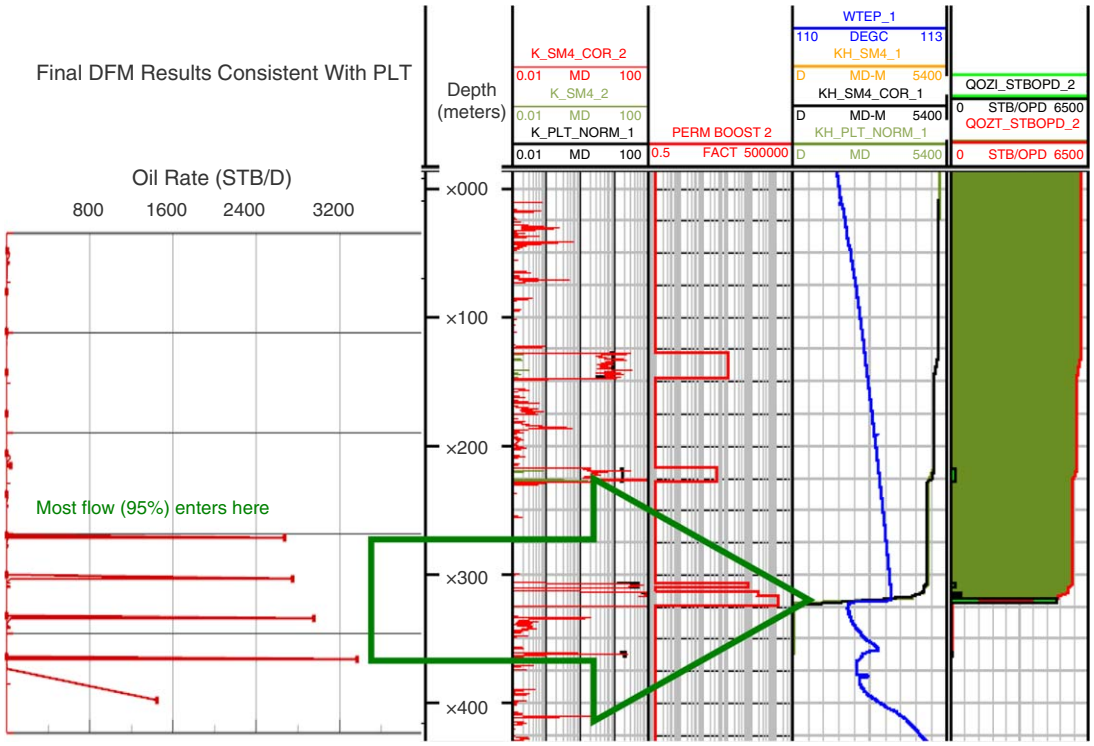


**Fig. 14—T-1 flow profile of one solution for Realization 5.**

the new result was moving in the direction as expected and in similar scale as predicted by the correlations, the same fracture realization was kept, and further iterations were continued. Because increasing $k_f$ 10 times led to the increase of $k^{\text{eff}}$ of six times, to adjust the outcome to 3.3 md, $k_f$ needed to be increased further at least three times.

The transient analysis of Case 2 numerical results provided the estimation of interporosity flow coefficient $\lambda$ as $3.2 \times 10^{-5}$, whereas the estimation from the gauge data was $2.8 \times 10^{-6}$. To reduce $\lambda$ 10 times, while increasing $k_f$ three times, the average $k_m$ needed to be decreased with a multiplier of 0.3 according to Eq. 3. Then, the input parameters of Case 3 were selected (Table 4).

The numerical results of Case 3 (blue curves in Fig. 13b) brought the estimations of $k^{\text{eff}}$ and $\lambda$ closer to the values derived from gauge data (Table 4). The obtained fracture storage ratio $\omega$ was 0.12. It needed to be increased to 0.22, the value from collected data. To do that, the fracture aperture would be doubled for the next case according to Eq. 2. Because $k^{\text{eff}}$ needed to be increased 1.3 times, from Eq. 1, $k_f$ would be decreased 0.8 times. The $\lambda$ value from Case 3 was $1.4 \times 10^{-5}$. To match the data with $\lambda$ of $2.8 \times 10^{-6}$, a multiplier of 0.3 for matrix permeability $k_m$ was needed based on Eq. 3.

After four iterations, the final numerical-model results (green curves) matched both the test history in Cartesian plot and the buildup pressure and pressure derivative data in log-log plot (Fig. 13c). The early-time response (before 2 hours after shut-in) departed from gauge data because the numerical model neglected wellbore-storage effects that were obvious in test data. After the wellbore storage was added, the numerical results could match the buildup data closely all the way to approximately 30 hours until offset-well production started to influence the test-well response.

This work-flow was successfully applied to integrate T-1 buildup-test data in the Tengiz discrete-fracture sector model. The flow profile at T-1 of the obtained numerical solution is consistent with the flow data from production logging, indicating that most of the flow enters the wellbore from a short-depth interval that corresponds with the location of a natural fracture **(Fig. 14).** The pressure results of the sector model are shown in **Fig. 15.** The biggest pressure change during buildup is in the northeast corner of the sector, indicating better fracture connectivity and interaction between matrix and fracture in that area.

Starting with the modified sector model that honors T-1 buildup data, a similar process was applied to Well T-2 in the same sector model. A buildup test conducted at T-2 in November 2008 shows DP transient behavior. The initial pressure field of the sector had to be transferred from the Tengiz full-field model at the beginning of that test. The fracture spacing and shape factor near T-2 were also calculated, which were different from those near T-1. The challenge in integrating T-2 transient data was that fracture Realization 5 could not provide enough fracture connectivity near T-2 to generate the expected pressure response. Except for fractures conditioned to match well-based observations, the specific locations of individual fractures throughout the reservoir in the discrete-fracture model are determined stochastically. Therefore, a new realization with more connected fractures around T-2 was created to repeat the procedure until a solution matching the buildup data reasonably well was found. This new sector model was then checked to validate that it still honored the buildup transient response at T-1. The sector properties were adjusted further to ensure consistency.

Because the properties in the well-drainage area have the dominant impacts on the pressure-transient responses at that well, to honor transient data collected at multiple wells, adjusting the numerical model parameters in the drainage area of each well respectively would provide consistent model solution. The drainage area could be estimated from several methods based on material balance (Kamal 2009). In our study, we calculated the area from the relative oil-production rate of each surrounding well and the PV near each well, and validated with the drainage area derived from the production-data analysis of long-term pressure and rate data.

## Integration of Pulse-Test Data

Just before the buildup test at T-2 in November 2008, a pulse test was conducted from T-2 to T-1. The oil-production history at the active Well T-2 during the pulse test is shown at the bottom of **Fig. 16,** which had five major rate changes to create the pulses. The observation Well T-1 was shut in and continuously

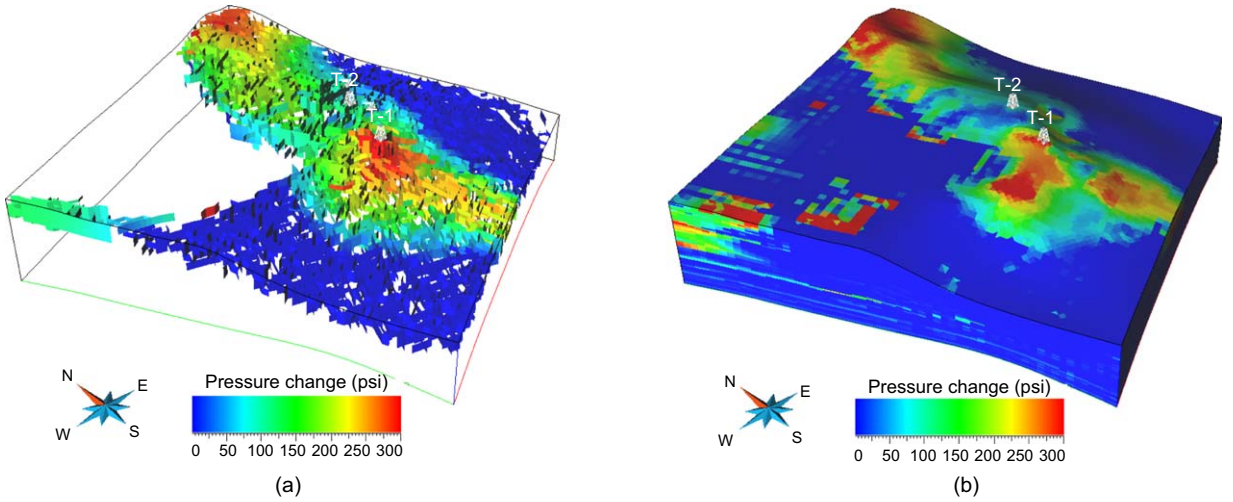


**Fig. 15—Simulated pressure change in (a) fracture and (b) matrix during 100-hour buildup of one solution for Tengiz sector-model Realization 5.**

collecting pressure responses shown at the top of Fig. 16. The correspondence between the pressure at T-1 and the production rate at T-2 is not obvious, but the pressure derivative with respect to time (the middle curve in Fig. 16) clearly indicates the direct correspondence between these two wells, implying good flow communication. The methods proposed by Deruyck et al. 1982 and Araujo et al. 1998 can be used to study the interference responses.

From synthetic case study, we learned that the dominant factors controlling pulse-signal propagation are the conductivity of the fractures connecting the two wells and the matrix porosity between the wells. This is consistent with previous reporting that the highest diffusivity medium controls the response between wells in multiple well testing (Woods 1970 and Kamal and Brigham 1975). Based on the sensitivity-study results, discrete-fracture model parameters were adjusted to honor pulse-test data from T-2 to T-1. Higher $k_f$ and lower $\phi_m$ would lead earlier responses to pulses. Starting with the green case of the modified fracture Realization 5, which matches buildup-test data from T-1 and T-2, the pulse-test responses between these two wells were generated **(Fig. 17),** which do not honor the measurements. Then, the fracture permeability was increased 12 times to generate the brown case, which has much quicker and bigger responses at T-1 than the measured data (red curve). Then, a smaller region around T-1 and T-2 in the northeast was selected, and its fracture permeability was increased to 1,000 darcies and the rest of the sector with the same fracture permeability of 28 darcies as the green case to generate the blue case, which matches the data reasonably well. In this example, the matrix porosity in the sector model remained the same as the green case. In other situations, it may be necessary to adjust both fracture permeability and matrix porosity in selected interference-test-influenced areas to match the pulse-test data. Using geological information (e.g., reservoir structure, facies, and fracture orientations) and model pressure-change maps could help to identify possible fast paths linking wells and the influence area of each test.

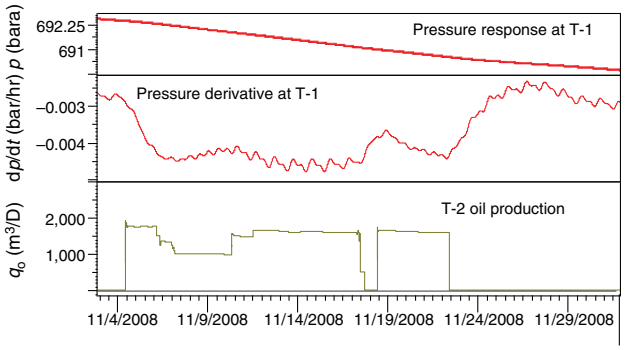


**Fig. 16—Pressure responses at Well T-1 to oil-production change at Well T-2 during pulse test in 2008.**

This new sector model was then checked for whether it still honored the buildup transient responses at T-1 and T-2. Further adjustments of the sector properties might be necessary to ensure consistency. For a full-field simulation study, the application of the proposed work-flow to honor individual well transient-test data and between-well pulse tests needs to be combined with global history matching to ensure material balance and the consistency with the long-term performance of the entire reservoir.

The benefits of dynamic transient-data integration include that it decouples the impacts of different formation properties, such as effective permeability, well skin factor, storativity ratio, and transmissibility between matrix and fracture; accelerates the data-matching process for the near-well local areas; and has the potential to reduce the efforts in long-term history matching with full-field simulation models.

## Conclusions and Discussions

1. NFR characterization is a complex problem with a high degree of uncertainty. A multidisciplinary team approach (spanning geology, field operation, well testing, and numerical simulation) is effective and necessary to solve a problem as challenging as NFR characterization. Having an effective reservoir surveillance plan in place and collecting all possible data of all types (well logs, cores, image logs, production log, single-well and multiple-well transient tests, and continuous downhole pressure and production rates) are crucial in obtaining reasonable characterization.
2. A deep understanding of fundamental flow behavior and proper calibration is needed before application to a full-field problem. Our study found that, for a numerical DPDK model, the grid size needs to be close to the fracture spacing in the reservoir near the well to be able to regenerate the representative interporosity-flow behavior. For a discrete-fracture model, first level of grid refinement is likely to reproduce the corresponding interporosity-flow signature.
3. Dynamic data contain valuable information that one should use to augment static data to improve reservoir characterization and to reduce uncertainty. A single-well drawdown/buildup test provides reservoir properties of the investigated local area, depending on the test duration. One can use pulse-test data to derive properties of the fast path or the most conductive layers between wells, and to provide information about reservoir connectivity.

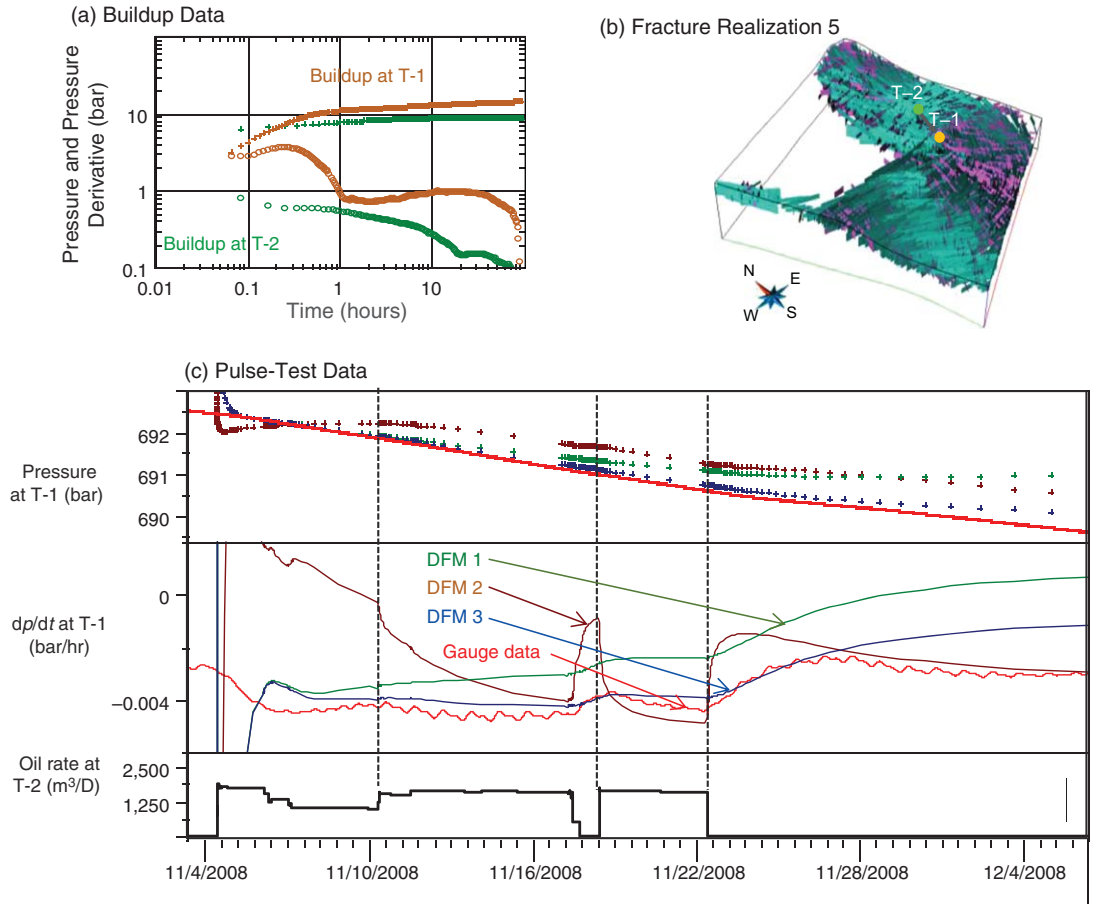


**Fig. 17—Integration of pulse test between T-2 and T-1 in Tengiz sector model.**

4. Theoretical/analytical solutions, when available, should always be used to guide numerical-simulation investigations. The representative fracture spacing and shape factor near a well in any model realizations can be derived by analyzing the numerically simulated transient-test responses and by comparing with the model input parameters. Depending on the fracture/matrix configurations near each well, the fracture spacing and shape factor may vary for different wells. These two parameters, together with the correlations, Eqs. 1 through 3, between the pressure-transient analysis results and the average model input parameters should be used to select the model input parameters for each iteration during the transient-data-matching process. This will reduce the number of iterations in numerical study.
5. The work-flow of transient-data integration was applied successfully in a sector model in the southeast of Tengiz field. From this field study, we learned that to honor buildup/drawdown test data collected at multiple wells, adjusting the numerical-model parameters in the drainage area of each well respectively would provide a consistent model solution. In certain situations, the fracture distribution at the first step of the work-flow may need to be changed to provide the needed connectivity before continuing with the rest of the steps in the work-flow. To match pulse-test data between wells, sometimes, it may require trial and error to identify the influence area and to adjust its dominant properties, such as fracture permeability and matrix porosity. The step-by-step integration procedure can be used to any NFRs with commercial pressure-transient-analysis software and numerical reservoir simulator.
6. A systematic procedure of integrating transient-test data in a numerical model combined with global history matching is expected to lead to an improved reservoir characterization. The steps are straightforward to follow, and should be applicable for most conditions of naturally fractured reservoirs. However, the application of a transient-data-integration work-flow in a large-scale full-field numerical-simulation model, and its impacts on the forecast of field performance need further study.

## Nomenclature

$a$ = aperture
$c$ = compressibility
$C$ = wellbore-storage coefficient
$h$ = sector-model thickness
$k$ = permeability
KSIGMA = product of matrix permeability and geometric shape factor
$L$ = individual-fracture length
$p$ = pressure
$q$ = flow rate
$r$ = wellbore radius
$s$ = well skin factor
$t$ = time
$x$ = fracture spacing
$\alpha$ = geometric shape factor in dual-porosity system
$\lambda$ = interporosity flow coefficient
$\omega$ = fracture storativity ratio
$\phi$ = porosity

### Subscripts

equiv = equivalent
$f$ = fracture
$m$ = matrix

$t$ = total
$w$ = well

**Superscript**
eff = effective

## Acknowledgments

The authors would like to thank Tengizchevroil and its partners, Chevron, ExxonMobil, KazMunayGas, and Lukoil, for the financial support and technical input for this work.

## References

Araujo, H. N., Andina, S. A., Gilman, J. R. et al. 1998. Analysis of Interference and Pulse Tests in Heterogeneous Naturally Fractured Reservoirs. Presented at the SPE Annual Conference and Exhibition, New Orleans, USA, 27–30 September. SPE-49234-MS. http://dx.doi.org/10.2118/49234-MS.

Barenblatt, G. I., Zheltov, Iu. P., and Kochina, I. N. 1960. Basic Concepts in the Theory of Seepage of Homogeneous Liquids in Fissured Rocks. *J. Appl. Math. Mech.* **24** (5): 1286–1303. http://dx.doi.org/10.1016/0021-8928(60)90107-6.

Basquet, R., Cohen, C. E., and Bourbiaux, B. 2005. Fracture Flow Property Identification: An Optimized Implementation of Discrete Fracture Network Models. Presented at the 14th SPE Middle East Oil and Gas Show and Conference, Bahrain, 12–15 March. SPE-93748-MS. http://dx.doi.org/10.2118/93748-MS.

Casabianca, D., Jolly, R. J. H., and Pollard, R. 2007. The Machar Oil Field: Waterflooding a Fractured Chalk Reservoir. *Geological Society, London, Special Publications* **270** (1): 171–191. http://dx.doi.org/10.1144/GSL.SP.2007.270.01.12.

Casciano, C., Ruvo, L., Volpi, B. et al. 2004. Well Test Simulation Through Discrete Fracture Network Modeling in a Fractured Carbonate Reservoir. *Petroleum Geoscience* **10** (4): 331–342. http://dx.doi.org/10.1144/1354-079303-590.

Coats, K. H. 1989. Implicit Compositional Simulation of Single-Porosity and Dual-Porosity Reservoirs. Presented at the SPE Symposium on Reservoir Simulation, Houston, USA, 6–8 February. SPE-18427-MS. http://dx.doi.org/10.2118/18427-MS.

Collins, J., Narr, W., Harris, P. M. et al. 2013. Lithofacies, Depositional Environments, Burial Diagenesis, and Dynamic Field Behavior in a Carboniferous Slope Reservoir, Tengiz Field (Republic of Kazakhstan), and Comparison With Outcrop Analogs. In *Deposits, Architecture, and Controls on Carbonate Margin, Slope, and Basinal Settings*, ed. K. Verwer, T. E. Playton, and P. M. Harris. SEPM Special Publication 105, 50–83.

Deruyck, B. G., Bourdet, D. P., DaPrat, G. et al. 1982. Interpretation of Interference Tests in Reservoirs With Double Porosity Behavior–Theory and Field Examples. Presented at the 57th SPE Annual Technical Conference and Exhibition, New Orleans, USA, 26–29 September. SPE-11025-MS. http://dx.doi.org/10.2118/11025-MS.

Hui, M. H., Kamath, J., Narr, W. et al. 2007. Realistic Modeling of Fracture Network in a Giant Carbonate Reservoir. Presented at the International Petroleum Technology Conference, Dubai, 4–6 December. SPE-11386-MS. http://dx.doi.org/10.2118/11386-MS.

Hui, M. H., Mallison, B., Lim, K. T. et al. 2008. An Innovative Workflow To Model Fracture in Tengiz Oil Field. Presented at the International Petroleum Technology Conference, Kuala Lumpur, 3–5 December. SPE-12572-MS. http://dx.doi.org/10.2118/12572-MS.

Hui, M. H., Mallison, B. T., Heidary-Fyrozjaee, M. et al. 2013. The Upscaling of Discrete Fracture Models for Faster, Coarse-Scale Simulations of IOR and EOR Processes for Fractured Reservoirs. Presented at the SPE Annual Technical Conference and Exhibition, New Orleans, USA, 30 September–2 October. SPE-166075-MS. http://dx.doi.org/10.2118/166075-MS.

Izadi, M. and Yildiz, T. 2009. Transient Flow in Discretely Fractured Porous Media. *SPE J.* **14** (2): 362–373. SPE-108190-PA. http://dx.doi.org/10.2118/108190-PA.

Kamal, M. M. and Brigham, W. E. 1975. Pulse-Testing Response for Unequal Pulse and Shut-in Periods. *SPE J.* **15** (5): 399–410. SPE-5053-PA. http://dx.doi.org/10.2118/5053-PA.

Kamal, M. M., Pan, Y., Landa, J. L. et al. 2005. Numerical Well Testing: A Method To Use Transient Testing Results in Reservoir Simulation. Presented at the SPE Annual Technical Conference and Exhibition, Dallas, USA, 9–12 October. SPE-95905-MS. http://dx.doi.org/10.2118/95905-MS.

Kamal, M. M. 2009. *Transient Well Testing*, SPE Monograph, Vol. 23. Richardson, Texas: SPE.

Karimi-Fard, M., Durlofsky, L. J., and Aziz, K. 2004. An Efficient Discrete Fracture Model Applicable for General-Purpose Reservoir Simulators. *SPE J.* **9** (2): 227–236. SPE-88812-PA. http://dx.doi.org/10.2118/88812-PA.

King, G. R., Jones, M., Dagistanova, K. et al. 2012. Use of Brownfield Experimental Design Methods for Post-Processing Conventional History Match Results. Presented at the SPE Annual Technical Conference and Exhibition, San Antonio, Texas, USA, 8–10 October. SPE-159341-MS. http://dx.doi.org/10.2118/159341-MS.

Lim, K. and Aziz, K. 1995. Matrix-Fracture Transfer Shape Factors for Dual-Porosity Simulators. *Journal of Petroleum Science and Engineering* **13:** 169–178. http://dx.doi.org/10.1016/0920-4105(95)00010-F.

Narr, W., Schechter, D. S., and Thompson, L. B. 2006. *Naturally Fractured Reservoir Characterization*. Richardson, Texas: Society of Petroleum Engineers.

Narr, W. and Flodin, E. 2012. Shallow-Burial Fractures in Steep-rimmed Carbonate Platforms: Outcrops in Canning Basin, NW Australia, as Analog for Tengiz Reservoir, Kazakhstan: Extended abs., Fundamental Controls on Flow in Carbonates. Presented at the AAPG Hedberg Conference, Saint-Cyr Sur Mer, Provence, France, 8–13 July.

Rogers, S., Enachescu, C., Trice, R. et al. 2007. Integrating Discrete Fracture Network Models and Pressure Transient Data for Testing Conceptual Fracture Models of the Valhall Chalk Reservoir, Norwegian North Sea. *Geological Society, London, Special Publications* **270** (1): 193–204. http://dx.doi.org/10.2118/GSL.SP.2007.270.01.13.

Samaniego-V, F. and Cinco-Ley, H. 2009. Chapter 10–Naturally Fractured Reservoirs, 221–280, Monograph Series No. 23. In *Transient Well Testing*, ed. M. M. Kamal. Richardson, Texas: SPE.

Sarma P. and Aziz, K. 2006. New Transfer Functions for Simulation of Naturally Fractured Reservoir With Dual-Porosity Models. *SPE J.* **11** (3): 328–340. SPE-90231-PA. http://dx.doi.org/10.2118/90231-PA.

Tankersley, T., Narr, W., King, G. R. et al. 2010. Reservoir Modeling To Characterize Dual Porosity, Tengiz Field, Republic of Kazakhstan. Presented at the SPE Caspian Carbonates Technology Conference, Atyrau, Kazakhstan, 8–10 November. SPE-139836-MS. http://dx.doi.org/10.2118/139836-MS.

Warren, J. E. and Root, P. J. 1963. The Behavior of Naturally Fractured Reservoirs. *SPE J.* **3** (3): 245–255. SPE-426-PA. http://dx.doi.org/10.2118/426-PA.

Wei, L., Hadwin, J., Chaput, E. et al. 1998. Discriminating Fracture Patterns in Fractured Reservoirs by Pressure Transient Test. Presented at the SPE Annual Technical Conference and Exhibition, New Orleans, USA, 27–30 September. SPE-49233-MS. http://dx.doi.org/10.2118/49233-MS.

Woods, E. G. 1970. Pulse-Test Response for a Two-Zone Reservoir. *SPE J.* **10** (3): 245–256. SPE-2570-PA. http://dx.doi.org/10.2118/2570-PA.

**Yan Pan** is a senior reservoir engineering adviser with Chevron Energy Technology Company. Her interest is focused on well testing, production-data analysis, and dynamic-data integration in reservoir models. Pan is the 2010 recipient of SPE Western North America Regional Formation Evaluation Award and served as a 2011–2012 SPE Distinguished Lecturer. She holds MS and PhD degrees in petroleum engineering from Stanford University.

**Mun-Hong Hui** is a research scientist with Chevron's Energy Technology Company based in San Ramon, California, and has 12 years of experience in the industry. He holds MSc/PhD degrees in petroleum engineering from Stanford University and a BEng degree in chemical engineering from the National University of Singapore. Hui's research interests are in the

simulation and upscaling of complex recovery physics, especially for NFRs.

**Wayne Narr** is senior research consultant for Chevron Energy Technology Company. He is a structural geologist, and his interest is focused on characterization of NFRs, ranging from analog studies to characterization methods to modeling. Narr has taught schools on NFRs and has published research articles on them as well as a book published by SPE. He holds a PhD degree from Princeton University, an MSc degree from University of Toronto, and a BS degree from Pennsylvania State University.

**Gregory King** is a reservoir engineer for Chevron. He is a coauthor of the 2001 SPE textbook, *Basic Applied Reservoir Simulation*, and the author or coauthor of more than 40 publications and technical papers. King holds BS, MS, and PhD degrees from the Pennsylvania State University, all in petroleum and natural-gas engineering. He has served on numerous SPE committees as a committee member or committee chair. King was awarded the SPE Regional Reservoir Dynamics and Description Award for the Russia and Caspian Region in 2014.

**Terrell H. Tankersley** is currently senior adviser geologist with Chevron Indonesia Company. He has been with Chevron-related companies for almost 35 years, focusing on development geology and reservoir modeling.

**Steve Jenkins is** development geologist with Karachaganak Petroleum Operating Company, Kazakhstan. He holds degrees in geology and geophysics, with an interest in climbing over and in carbonate outcrops.

**Eric Flodin** is currently Earth science adviser at Chevron Pacific Indonesia in Minas, Sumatra, Indonesia. Prior roles include development geologist at Tengizchevroil, fractured-reservoir consultant at Chevron Energy Technology Company, and faculty in the Geosciences Department, Indiana University/Purdue University, Fort Wayne. Flodin holds a BS degree in geology from Indiana University/Purdue Univeristy, Indianapolis and a PhD degree in geology from Stanford University.

**Philip W. Bateman** is currently the Gorgon Subsurface Manager for Chevron, and his previous position was Asset Development Manager for Tengizchevroil. He has been with Chevron for 27 years. Bateman's interests include carbonate and fractured reservoir characterization, petrophysics, and reservoir-modeling work flows. He holds a PhD degree in geology from the Colorado School of Mines. Bateman is a member of SPE.

**Chris Laidlaw** is a deputy asset manager for Chevron Thailand. He has been with Chevron for 28 years, working in multiple international locations. Laidlaw's professional interests are in reservoir management and subsurface asset development. He holds an MSc degree in petroleum engineering from Imperial College, London.

**Hai Vo** currently works for Chevron Energy Technology Company. He holds MS and PhD degrees, both in petroleum engineering, and a PhD degree minor in computational mathematics from Stanford University. Vo's research interests include reservoir characterization and field-production optimization.